Mathematical
Institute

Peter Julius Waldert, BSc BSc

General Kernel Spectral Methods for Equilibrium Measures

MASTER'S THESIS

a thesis submitted for the degree of

Master of Science (MSc)

in

Mathematical Modelling and Scientific Computing (MMSC)

submitted to the

University of Oxford

Academic Supervisors

Dr. Timon Gutleb[a]
Prof. José A. Carrillo de la Plata MA, FEurASc, FSIAM, MAE, FIMA[a]

[a]Mathematical Institute, University of Oxford

Oxford, August 2023

Abstract

To be written.

This MMSC thesis will further explore general kernel spectral methods for finding equilibrium measures where initial progress made in Gutleb, José A. Carrillo and S. Olver 2022b and Gutleb, José A. Carrillo and S. Olver 2022a.

Statement of Originality: The extension of the attractive-repulsive kernel spectral method into a general kernel spectral method along with an implementation of it is original. All code contributions, starting from the particle simulation software to the implementation of the spectral methods, are entirely original.

Keywords: Pairwise Interaction Potentials, Many-Body Systems, Particle Simulations, Swarming Behaviours, Equilibrium Measures, Spectral Methods, Orthogonal Polynomials

Languages: C++, Julia, Python

Contents

Chapter 1

Introduction

This chapter will give a brief overview of the setting of the problem considered in this dissertation, motivate a few biological and physical examples, and set up some notational conventions.

1.1 Problem Setting

The present thesis is concerned with many-body systems, treating particles in an abstract sense as they could take the form of physical atoms, birds in a flock or fish in a school. Other examples include ant colonies and swarms of insects such as locusts. A swarm of animals, a set of coordinated entities, brings many advantages for its members. For example, they share water resistance or it is easier to find a mate within the swarm than otherwise. They also often mimic larger animals to fend off predators and swarming behaviour ("swarm intelligence") plays an important role in this process. There are some disadvantages as well, like the accelerated spread of diseases or when resources are scarce, some swarm species even begin cannibalistic behaviour (D'Orsogna 2017).

From a more physical perspective, pair potentials $K : \mathbb{R}^+ \mapsto \mathbb{R}$ provide a simple and computationally efficient way to approximate the interaction between two particles based solely on their distance (cf. Figure 1.1a as a simple illustration). Pairwise potentials can be used to approximate a wide range of interactions, including interatomic potentials in physics and computational chemistry. Common examples of pair potentials include the Lennard-Jones potential and the Morse potential, which are widely used in molecular dynamics simulations to study the behavior of atoms and

molecules, as well as the Coulomb potential used to describe the interaction between two charges in electrodynamics.

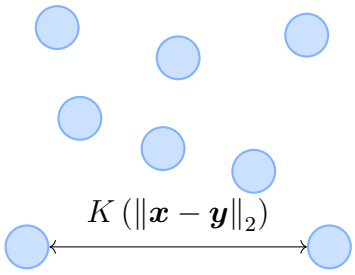

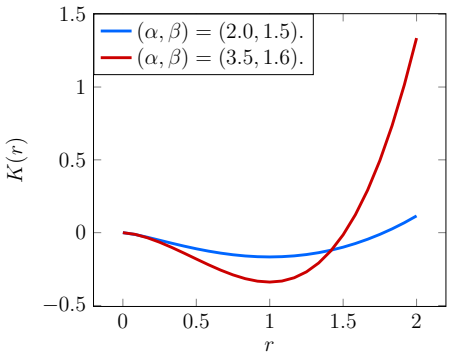

(a) $N = 8$ particles interacting with one another through the potential $K(r)$.

(b) Plot of attractive-repulsive potential functions $K_{\alpha,\beta}(r) = \frac{r^\alpha}{\alpha} - \frac{r^\beta}{\beta}$ for different α, β.

From here on, we will refer to said swarm entities, be it fish, birds or atoms, as *particles*.

1.2 Notational Conventions

Let $\mathbb{N}$ denote the natural numbers (positive integers) without 0 and let $\mathbb{N}_0 := \mathbb{N} \cup \{0\}$. In the following, we will use **bold** notation for vectors, matrices will generally be denoted by a capital letter and scalars by a lowercase letter. We will frequently make use of the (Euclidean) 2-norm of a vector, as denoted by $\|\cdot\|_2$. So for a d-dimensional vector $\boldsymbol{x} \in \mathbb{R}^d$ we have $\|\boldsymbol{x}\|_2 := \sqrt{\sum_{k=1}^d x_k^2}$. Also note that for readability, we will use the notation $\boldsymbol{x}^2 := \boldsymbol{x}^T\boldsymbol{x} = \|\boldsymbol{x}\|_2^2 \in \mathbb{R}^+$.

One should also clarify the nature of a few of the integrals appearing in this thesis which are often performed over the closed unit ball $B_1(\boldsymbol{x}) := \{\boldsymbol{y} \in \mathbb{R}^d \mid \|\boldsymbol{x}-\boldsymbol{y}\|_2 \leq 1\}$ centered at the origin $\boldsymbol{x} = \boldsymbol{0}$. These volume integrals (often ended by $\mathrm{d}^d y$ or $\mathrm{d}V$) over the d-dimensional unit ball shall be written as

$$\int_{B_1(\boldsymbol{0})} \mathrm{d}\boldsymbol{y}\,,$$

where $\boldsymbol{y} \in \mathbb{R}^d$ is the integration variable. Note that some definitions of $B_1(\boldsymbol{x})$ are open sets, leaving out the shell $\{\boldsymbol{y} \in \mathbb{R}^d \mid \|\boldsymbol{x}-\boldsymbol{y}\|_2 = 1\}$. The choice of definition does not matter for our purposes as the shell, a hyperplane of Lebesgue measure 0, does not contribute to the integral.

All numerical plots and figures in this thesis were generated using the Makie visualisation tool (Danisch and Krumbiegel 2021), an open-source package available for the Julia computing language (Bezanson et al. 2017).

Just Notes

This chapter's purpose is the collection of notes, and it will not be included in the final dissertation.

Special Functions we like

Pochhammer's falling symbol $(x)_n := \prod_{k=0}^{n-1}(x-k)\,.$

Pochhammer's rising symbol $(x)^n := \prod_{k=0}^{n-1}(x+k)\,.$

Generalised hypergeometric series

$$ {}_pF_q(a_1,\ldots,a_p;b_1,\ldots,b_q;z) := \sum_{n=0}^{\infty} \frac{(a_1)_n\cdots(a_p)_n}{(b_1)_n\cdots(b_q)_n}\,\frac{z^n}{n!}\,. $$

(Gaussian) Hypergeometric function

$$ {}_2F_1(a,-n;c;z) = \sum_{j=0}^{n}(-1)^j \binom{n}{j} \frac{(a)_j}{(c)_j} z^j\,. $$

(A special case of the hypergeometric series with $p=2$, $q=1$).

Jacobi (=hypergeometric) polynomials

$$ P_n^{(\alpha,\beta)}(z) := \frac{(\alpha+1)_n}{n!}\,{}_2F_1\left(-n,1+\alpha+\beta+n;\alpha+1;\tfrac{1}{2}(1-z)\right)\,. $$

Gegenbauer (=ultraspherical) polynomials

$$ C_n^{(\lambda)}(z) := \frac{(2\lambda)_n}{n!}\,{}_2F_1\left(-n,2\lambda+n;\lambda+\frac{1}{2};\frac{1-z}{2}\right) = \frac{(2\lambda)_n}{(\lambda+\frac{1}{2})_n} P_n^{(\lambda-1/2,\lambda-1/2)}(x)\,. $$

They satisfy a three-term recurrence relation (as all orthogonal polynomials do!)

$$\begin{aligned} C_0^{(\lambda)}(x) &= 1 \\ C_1^{(\lambda)}(x) &= 2\lambda x \\ (n+1)C_{n+1}^{(\lambda)}(x) &= 2(n+\lambda)xC_n^{(\lambda)}(x) - (n+2\lambda-1)C_{n-1}^{(\lambda)}(x). \end{aligned} \quad .$$

From Wikipedia: In spectral methods for solving differential equations, if a function is expanded in the basis of Chebyshev polynomials and its derivative is represented in a Gegenbauer/ultraspherical basis, then the derivative operator becomes a diagonal matrix, leading to fast banded matrix methods for large problems (S. Olver and Townsend 2013).

Three-term recurrence relationship F. Olver et al. 2018, p. 18.9.1:

$$xC_n^{(\lambda)}(x) = \tfrac{(n+2\lambda-1)}{2(n+\lambda)}C_{n-1}^{(\lambda)}(x) + \tfrac{n+1}{2(n+\lambda)}C_{n+1}^{(\lambda)}(x). \tag{1.1}$$

1.2.1 Theorem: Two term recurrence of Q^α

The integral operator

$$Q^\alpha\left[u\right](x) = \int_{-1}^{1} |x-y|^\alpha u(y)\,\mathrm{d}y$$

satisfies a two-term recurrence relationship when acting on the ultraspherical polynomials $C_n^{(\lambda)}(y)$ with weight $w(y) = (1-y^2)^{\lambda-\frac{1}{2}}$ such that

$$xQ^\alpha\left[wC_n^{(\lambda)}\right](x) = \kappa_1 Q^\alpha\left[wC_{n-1}^{(\lambda)}\right](x) + \kappa_2 Q^\alpha\left[wC_{n+1}^{(\lambda)}\right](x),$$

where $n \geq 2$ and with the constants

$$\begin{aligned} \kappa_1 &= \frac{(n-\alpha-1)(2\lambda+n-1)}{2n(\lambda+n)}, \\ \kappa_2 &= \frac{(n+1)(2\lambda+n+\alpha+1)}{2(\lambda+n)(2\lambda+n)}. \end{aligned}$$

Chapter 2

Particle Interaction Theory

As mentioned in the introduction.

Definition: An N_p-Body System is a set of particles with position and velocity interacting with one another. Each particle individually is subject to inertia and its kinetic energy ("second moment" [1]) is given by

$$E_{\text{kin},i} = \frac{\boldsymbol{p_i}^2}{2m} = \frac{(m\boldsymbol{v_i})^2}{2m} = \frac{1}{2} m \left\|\boldsymbol{v_i}\right\|_2^2 .$$

The second important ingredient is an interaction potential motivating pairwise forces $\boldsymbol{F_{ij}} \in \mathbb{R}^d$ between particles

$$\boldsymbol{F}_{ij} = -\nabla U_{ij} = -\left(\partial x_1, ..., \partial x_d\right)^T U_{ij} .$$

The total potential of a system of $N_p \geq 2$ particles $U \in \mathbb{R}$ can be calculated by summing up the pair potentials $U_{ij} \in \mathbb{R}$ between all pairs of particles

$$U = \sum_{i=1}^{N_p} \sum_{j=1, j\neq i}^{N_p} U_{ij} = \sum_{i=1}^{N_p} \sum_{j=1, j\neq i}^{N_p} K\left(\left\|\boldsymbol{x_i} - \boldsymbol{x_j}\right\|_2\right) ,$$

where $\boldsymbol{x_i} \in \mathbb{R}^d$ represents the d-dimensional position of particle i, respectively. An example we will study is that of an attractive-repulsive interaction potential, where two power-law potentials compete with each other. For a given $\alpha, \beta \in \mathbb{R}\backslash\{0\}$, it is given by

$$K_{\alpha,\beta}(r) = \frac{r^\alpha}{\alpha} - \frac{r^\beta}{\beta} .$$

[1] In kinetic theory, the 0th moment is the mass m_i of a particle, the first moment is the momentum $\boldsymbol{p_i}$ and the second moment is its kinetic energy $E_{kin,i}$.

One can even consider the case where either α or β is 0 in order to arrive at a log-term (José A. Carrillo and Huang 2017), using the convention that $\frac{x^0}{0} := \log(x)^2$. If the repulsive term is stronger (so $\beta > \alpha$), there is no equilibrium distribution as particles simply continue repelling each other out to infinity.

The Lennard-Jones potential ($\alpha = -12, \beta = -6$), for example, is an **intermolecular** potential, so the relevant length-scale is between molecules. Therefore, the only relevant interaction is the electromagnetic force. Other forces, such as strong force which keeps protons in the nucleus together (a force much stronger than the electromagnetic one, but with much lower reach), need not be considered at this length-scale.

In the absence of an external potential V, the total energy is given by $E = E_{\text{kin}} + U$, so

$$E = \frac{1}{2}\sum_{i=1}^{N_p} m_i \boldsymbol{v_i}^2 + \sum_{i=1}^{N_p}\sum_{j=1, j\neq i}^{N_p} K\left(\|\boldsymbol{x_i} - \boldsymbol{x_j}\|_2\right) . \tag{2.1}$$

Each particle $i = 1, ..., N_p$ at position $\boldsymbol{x_i} \in \mathbb{R}^d$ and time $t \in \mathbb{R}^+$ then follows

$$\frac{\mathrm{d}^2 \boldsymbol{x_i}}{\mathrm{d}t^2} = f\left(\left\|\frac{\mathrm{d}\boldsymbol{x_i}}{\mathrm{d}t}\right\|_2\right)\frac{\mathrm{d}\boldsymbol{x_i}}{\mathrm{d}t} - \frac{1}{N}\sum_{j=1, i\neq j}^{N} \nabla K\left(\|\boldsymbol{x_i} - \boldsymbol{x_j}\|_2\right) , \tag{2.2}$$

for reference see, for example, (Gutleb, José A. Carrillo and S. Olver 2022b; Gutleb, José A. Carrillo and S. Olver 2022a). For now, we only consider the case without an external potential $V(\boldsymbol{x})$.

2.1 Continuous Limit

The evolution equation, in the continuous limit as $N_p \to \infty$, becomes

$$\frac{\partial \rho}{\partial t} = \nabla \cdot (\rho \nabla K * \rho) . \tag{2.3}$$

where $\rho : \mathbb{R} \mapsto \mathbb{R}$ is the particle density function.

Proof. **To be included.**

□

[2]Consider the Laurent series expansion of $\frac{x^a}{a} = \frac{1}{a} + \log(x) + \frac{1}{2}a\log^2(x) + \mathcal{O}(a^2)$ in the limit as $a \to 0^+$. While this limit approaches ∞ coming from the right and $-\infty$ coming from the left due to the nature of the first term in the expansion, the only remaining term in it is $\log(x)$ which is thereby chosen as a convention.

The solution ρ we are looking for within the scope of this dissertation is the *equilibrium measure* (cf. Definition 2.1.1) minimizing the total potential U.

2.1.1 Definition: Equilibrium Measure

For a given pairwise interaction potential $K : \mathbb{R} \mapsto \mathbb{R}$, the equilibrium measure $\rho : \mathbb{R} \mapsto \mathbb{R}$ is a measure chosen such that

$$U = \frac{1}{2} \iint K\left(\|\boldsymbol{x} - \boldsymbol{y}\|_2\right) \, \mathrm{d}\rho(\boldsymbol{x}) \, \mathrm{d}\rho(\boldsymbol{y}) \,,$$

is minimised, where $\mathrm{d}\rho = \rho(\boldsymbol{x})\mathrm{d}\boldsymbol{x}$.

Also consider the total mass of the equilibrium distribution, given by

$$M = \int \mathrm{d}\rho = \int_{\mathrm{supp}(\rho)} \rho(\boldsymbol{x}) \, \mathrm{d}\boldsymbol{x} \,, \tag{2.4}$$

which, without loss of generality, we can choose as $M = 1$ to make $\rho(\boldsymbol{x})$ a *probability distribution*.

2.2 Self-Propulsion

Makes it active matter. Self-propulsion and friction could be modelled as a quadratic of the form

$$f(v_i) = 1.6 - 0.5 v_i^2 \,,$$

where $v_i := \|\boldsymbol{v_i}\|_2 = \left\| \frac{\mathrm{d}\boldsymbol{x_i}}{\mathrm{d}t} \right\|_2$.

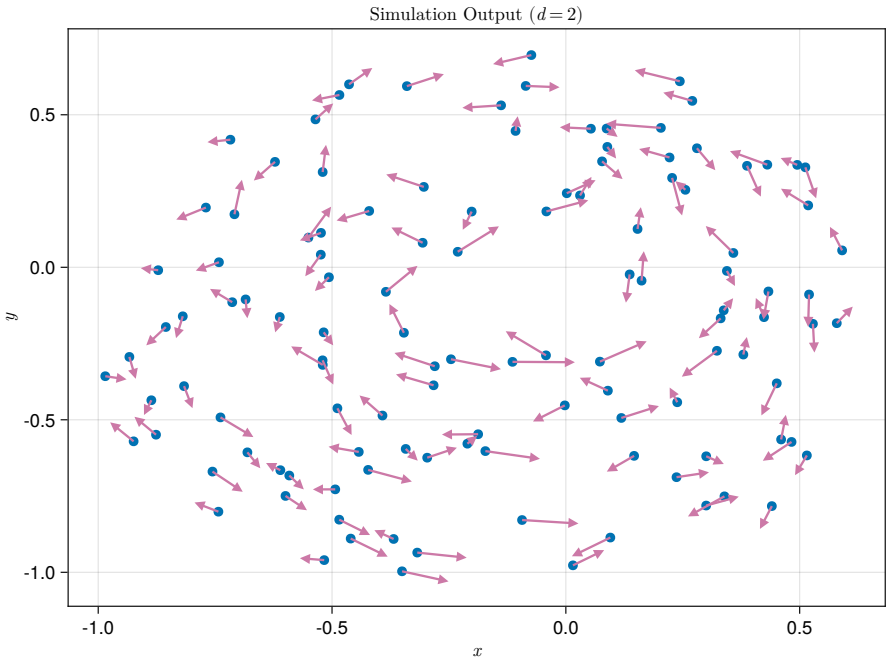

Figure 2.1: Position and velocity of particles in the simulation. Reproduced plot from D'Orsogna et al. 2006.

To be included.

2.3 Kinetic Theory: The Vlasov Equation

A very common tool in Plasma physics.

$$\frac{\partial f}{\partial t} + \frac{\mathrm{d}\mathbf{r}}{\mathrm{d}t} \cdot \frac{\partial f}{\partial \mathbf{r}} + \frac{\mathrm{d}\mathbf{p}}{\mathrm{d}t} \cdot \frac{\partial f}{\partial \mathbf{p}} = 0,$$

This is the collisionless Boltzmann equation. Vlasov replaces the collision term with long-range interactions.

2.3.1 Theorem: Liouville's

Says that phase-space volume is conserved in situations of a pure particle-particle interaction.

$$\frac{d\rho}{dt} = \frac{\partial \rho}{\partial t} + \sum_{i=1}^{n} \left(\frac{\partial \rho}{\partial q_i} \dot{q}_i + \frac{\partial \rho}{\partial p_i} \dot{p}_i \right) = 0\,.$$

2.4 Vicsek Model

For the study of active matter (a number of individual agents).

2.5 Swarming

A 2010 paper by Cavagna et al. showed the surprising result that correlation between movement of individual starlings in bird flocks over Rome is scale-free. In contrast to the assumption that birds only mirror their neighbours' behaviour and swarming behaviour emerges as a result of that, this observation suggests that bird flocks exert collective behaviour beyond local interactions.

> The change in the behavioral state of one animal affects and is affected by that of all other animals in the group, no matter how large the group is (Cavagna et al. 2010).

This work was done by individually tracking each starling in the flock and using tracking algorithms to represent their 3 dimensional positions and velocities.

Chapter 3

Particle Simulator

The aforementioned many-body systems generally exert very complex behaviour when viewed as a whole. This behaviour can be captured in mathematical terms but also from a simulation perspective. Particle simulations have been a subject of much attention in physics and scientific computing more generally. This class of simulations, in the context of intermolecular interactions, is often referred to as molecular dynamics.

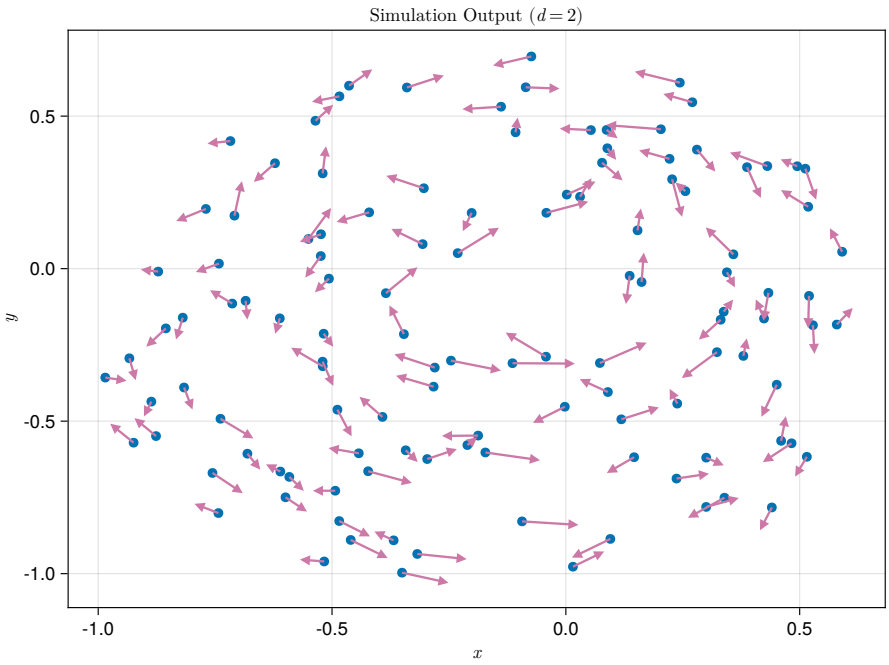

Figure 3.1: Position and velocity of particles in the simulation at a point in time. Every particle, each of equal mass m, interacts with every other particle through the interaction potential $U_{ij} = K\left(\|\boldsymbol{x_i} - \boldsymbol{x_j}\|_2\right)$ leading to $\mathcal{O}(N_p^2)$ interactions.

Because each particle interacts with every other particle, the number of interactions scales with $\mathcal{O}(N_p^2)$, which can play a prohibitive role in terms of the computation time when increasing the number of particles $N_p \gg 1$.

Within the scope of this thesis, in order to understand the elaborate behaviour of such particle systems and also to verify results from theory and the spectral method, we provide an implementation of a simulator starting from a numerical time integrator in $\mathbb{R}^d$. In addition to the *headless* simulation software, exporting state and results for treatment by the analysis component, a Graphical User Interface (GUI) is provided to enable live insight into and interaction with the model.

Figure 3.2: Screenshot of the GUI provided for the particle simulator. The top row shows the position of particles in their $[-1, 1]^d$ domain at a point t in time, the energy development over time and the current position/velocity phase space plot. Below, there are position and velocity histogram updated live along with the simulation.

3.1 Available Methods

- Simple Forward Integration
- Multistep Methods, which is an extension to the simple integration above.
- Fast Multipole Method
- Multigrid Methods

3.1.1 Leapfrog Integration

Nice introduction here. Maybe compare with Advanced HMC?

To be included.

3.2 Phase Space

Each particle, at every point in time t, has a position and velocity value. In $d = 1$ dimension, one can visualise both of these quantities simultaneously in a phase space plot (cf. Section 3.2). For $d > 1$ dimension, it is possible to either only visualise the first components $\{\boldsymbol{x_i}\}_1$ and $\{\boldsymbol{v_i}\}_1$ or to visualise the norm of the position (distance from the center of mass) $\|\boldsymbol{x_i} - \boldsymbol{x}_{\text{center}}\|_2$ and velocity $\|\boldsymbol{v_i}\|_2$, where

$$\boldsymbol{x}_{\text{center}} := \frac{1}{N_p} \sum_{i=1}^{N_p} \boldsymbol{x_i} \, .$$

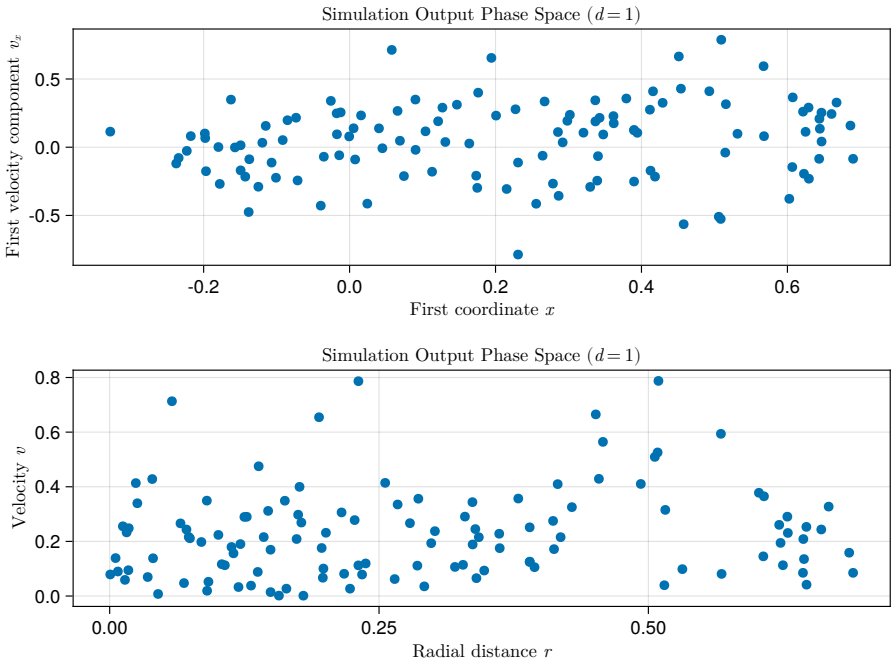

Figure 3.3: Position and velocity of particles in the simulation visualised as a phase space plot.

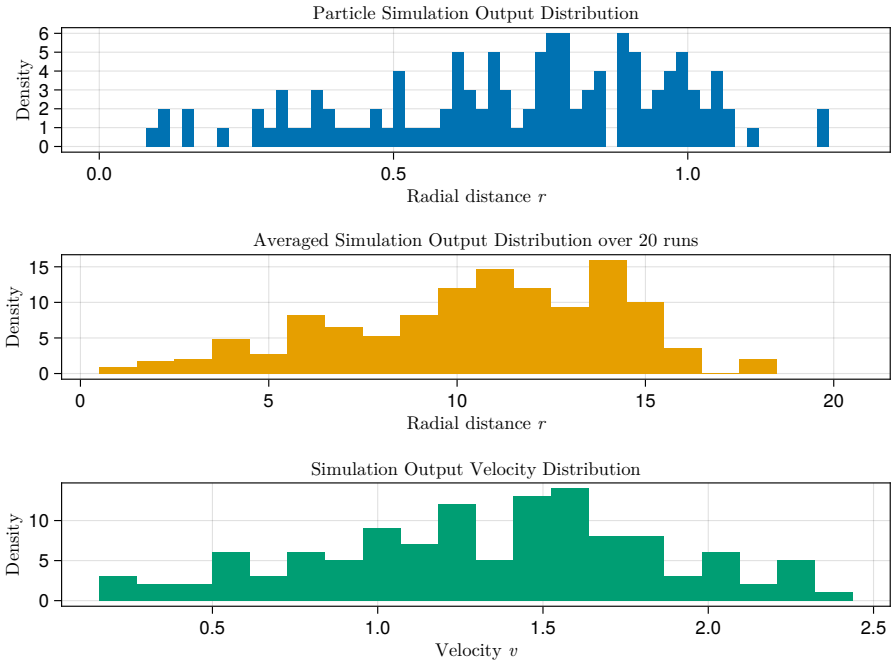

Figure 3.4: Position Histogram

Chapter 4

Spectral Method

4.1 Content

solves an [[Integral Equation]] or [[Differential Equation]] by assuming a solution of the form

$$\rho(x) = \sum_{k=1}^{N} \rho_k b_k(x)$$

where $\{b_k\}$ is a basis of functions.

4.1.1 Structure

- Introduce [[Chebyshev Polynomials]], [[Gegenbauer Polynomials|Ultraspherical Polynomials]], [[Jacobi Polynomials]], etc.
- Describe the method
- Talk about the resulting [[Operator]].
  - [[Derivation of In-Operator Recurrence]]
- Numerical Analysis ([[Bound on the Error]])
- Show results here? Or in extra results chapter?

4.2 Definitions

4.2.1 Definition: Ansatz

$$\rho(\boldsymbol{x}) = \left(1 - \|\boldsymbol{x}\|_2^2\right)^{m-\frac{\alpha+d}{2}} \sum_{k=1}^{N} P_k^{(a,b)}(2\|\boldsymbol{x}\|_2^2 - 1)$$

4.2.2 Definition: Bound on the Error

- [ ] How does one look at this topic? We should have [[Spectral Convergence]], hopefully.

4.2.3 Definition: Chebyshev Polynomials

Of the first kind:

$$T_k(x)$$

Of the second kind:

$$U_k(x)$$

Also have a [[Three-Term Recurrence Relationship]].

Based on the Three-Term Recurrence Relationship (cf. Definition 4.2.15).

One can even determine an explicit relationship between the coefficients in the Jacobi expansion by considering the Jacobi Matrix (cf. Definition 4.2.9).

Considering the operator $\hat{Q}^\beta[\rho]$ as in Theorem 4.2.1, from the ansatz $\rho(\boldsymbol{x})$ (cf. Definition 4.2.1) we have

$$\hat{Q}^\beta(x) = \sum_{k=0}^{N-1} \rho_k \int_{B_1(\mathbf{0})} \|\boldsymbol{x}-\boldsymbol{y}\|_2^\beta \left(1-\|\boldsymbol{y}\|_2^2\right)^a P_k^{(a,b)}\left(2\|\boldsymbol{y}\|_2^2-1\right) \mathrm{d}\boldsymbol{y}\,. \tag{4.1}$$

We are now interested in a numerical representation of the operator $\hat{Q}^\beta$ acting on the function $\rho \in L^2$, so an equivalent (linear) operator $Q^\beta : \mathbb{R}^N \mapsto \mathbb{R}^N$ acting on the coefficients $\rho_k \in \mathbb{R}$, $k = 1, ..., N$. As every finite-dimensional linear operator must have a matrix representation, we are looking for a $Q^\beta \in \mathbb{R}^{N\times N}$ such that

$$\hat{Q}^\beta[\rho](\boldsymbol{x}) = \boldsymbol{P}_k^{(a,b)}\left(2\|\boldsymbol{x}\|_2^2-1\right)\cdot Q^\beta\boldsymbol{\rho}\,,$$

where $\boldsymbol{P}_k^{(a,b)}\left(2\|\boldsymbol{x}\|_2^2-1\right) \in \mathbb{R}^N$ is the vector of Jacobi polynomials $P_0^{(a,b)}(x)$, $P_1^{(a,b)}(x)$, ..., $P_{N-1}^{(a,b)}(x)$ evaluated at $2\|\boldsymbol{x}\|_2 - 1$ as introduced in and after Definition 4.2.10.

Therefore, starting from Equation (4.2), we obtain

$$\begin{aligned}\hat{Q}^\beta[\rho](\boldsymbol{x}) &= \sum_{k=0}^{N-1}\rho_k\hat{Q}^\beta[wP_k](\boldsymbol{x}) = \sum_{k=0}^{N-1}\rho_k\sum_{j=0}^{N-1} q_{kj}P_k^{(a,b)}\left(2\|\boldsymbol{x}\|_2^2-1\right)\\ &= \sum_{j=0}^{N-1}\sum_{k=0}^{N-1}\rho_k q_{kj}P_k^{(a,b)}\left(2\|\boldsymbol{x}\|_2^2-1\right)\,,\end{aligned}$$

which we will rewrite in matrix-form,

$$\begin{aligned}\hat{Q}^\beta[\rho](\boldsymbol{x}) &= \boldsymbol{P}(\boldsymbol{x})\cdot\begin{pmatrix}\sum_{k=0}^{N-1}\rho_k q_{k,1}\\ \vdots\\ \sum_{k=0}^{N-1}\rho_k q_{k,N}\end{pmatrix} = \boldsymbol{P}(\boldsymbol{x})\cdot\underbrace{\begin{pmatrix}q_{11} & \cdots & q_{1N}\\ \vdots & \ddots & \vdots\\ q_{N1} & \cdots & q_{NN}\end{pmatrix}}_{=:Q^\beta}\begin{pmatrix}\rho_0\\ \vdots\\ \rho_{N-1}\end{pmatrix}\\ &= \boldsymbol{P}_k^{(a,b)}\left(2\|\boldsymbol{x}\|_2^2-1\right)\cdot Q^\beta\boldsymbol{\rho}\end{aligned}$$

where we used $\boldsymbol{P}(\boldsymbol{x}) = \boldsymbol{P}_k^{(a,b)}\left(2\|\boldsymbol{x}\|_2^2-1\right)$ as a shorthand giving us the form of the operator matrix. Each value q_{kj} in it is therefore chosen to satisfy

4.2.4 Definition: Function Space

To be defined, but the space our coefficients are in. Could be

$$L^2 := \{f : \mathbb{R} \mapsto \mathbb{R} | f \text{ square integrable?}\}$$

4.2.5 Definition: Gaussian Hypergeometric Function

Written as

$${}_2F_1(a, b; c; z)$$

4.2.6 Definition: Gegenbauer Polynomials

alias: Ultraspherical Polynomials
Are a special case of the Jacobi Polynomials (cf. Definition 4.2.10) and form an Orthonormal Basis (cf. **??**) under the weight given by

$$w(x) = (1 + x)^\alpha$$

4.2.7 Definition: Generalised Hypergeometric Series

Is given by

$${}_pF_q$$

Special Case: [[Gaussian Hypergeometric Function]]. The definition involves the Rising Factorial (cf. Definition 4.2.13) (Pochhammer Symbol).

4.2.8 Definition: Integration Routine

Could be done using Cubature. Otherwise, just Forward Euler.

4.2.9 Definition: Jacobi Matrix

aliases: Jacobi Operator
The Jacobi operator is the matrix $X \in \mathbb{R}^{N \times N}$ satisfying

$$x \cdot P(x) = P(x) \cdot X^T$$

4.2.10 Definition: Jacobi Polynomials

Let $P^{(a,b)} : \mathbb{C} \mapsto \mathbb{C}$ with

$$P_n^{(a,b)}(x) = \frac{(a+1)_n}{n!}\, {}_2F_1\left(-n, 1+a+b+n; a+1; \tfrac{1}{2}(1-x)\right)$$

So are defined using the Gaussian Hypergeometric Function (cf. Definition 4.2.5) and the Pochhammer symbol. Which is equivalent to

$$P_n^{(a,b)}(x) = \frac{\Gamma(a+n+1)}{n!\,\Gamma(a+b+n+1)} \sum_{m=0}^{n} \binom{n}{m} \frac{\Gamma(a+b+n+m+1)}{\Gamma(a+m+1)} \left(\frac{x-1}{2}\right)^m .$$

where $\Gamma(x) = \int_0^\infty t^{x-1} e^{-t}\, \mathrm{d}t$ (with $\mathfrak{Re}(x) > 0$) is the gamma function [1]. Gegenbauer Polynomials (cf. Definition 4.2.6) are a special case. And Chebyshev Polynomials (cf. Definition 4.2.3) are a special case of them.

Following from this definition,

$$P_0^{(a,b)}(x) = 1$$
$$P_1^{(a,b)}(x) = (a+1) + (a+b+2)\frac{x-1}{2}$$

and so on. Note that obviously, $\deg\left(P_k^{(a,b)}\right) = k$.

4.2.1 Nice Spectral Properties

- Differentiation
- Three-Term Recurrence
- why are they better than just Chebyshev?

Note that in this manuscript we will use the dot-product notation

$$f(x) = \sum_{k=0}^{N-1} f_k P_k^{(a,b)}(x) \quad \Leftrightarrow \quad f(x) = \boldsymbol{f} \cdot \boldsymbol{P}^{(a,b)}(x)\,,$$

to express that a function f is a linear combination of basis polynomials with coefficients $\boldsymbol{f} = (f_0, ..., f_{N-1})^T \in \mathbb{R}^N$. So $\boldsymbol{P}^{(a,b)}(x) \in \mathbb{R}^N$ is the vector of Jacobi polynomials $P_0^{(a,b)}(x)$, $P_1^{(a,b)}(x)$, ..., $P_{N-1}^{(a,b)}(x)$.

Jacobi polynomials $P_n^{(a,b)}(x)$ are orthogonal on $[-1, 1]$ w.r.t. the weight function

$$w^{(a,b)}(x) = (1-x)^a (1+x)^b\,,$$

[1] Recall that for integer arguments $k \in \mathbb{N}$, it equals the factorial of $(k-1)$ so $\Gamma(k) = (k-1)!$.

so they satisfy

$$\int_{-1}^{1}(1-x)^a(1+x)^b P_n^{(a,b)} P_m^{(a,b)}\,\mathrm{d}x = \frac{2^{a+b+1}\Gamma(a+n+1)\Gamma(b+n+1)}{n!(a+b+2n+1)\Gamma(a+b+n+1)}\delta_{n,m}\,,$$

with $a, b > -1$, which uniquely determines $P_n^{(a,b)}(x)$. The special case of $a = b$ corresponds to the ultraspherical or Gegenbauer polynomials, while the case $a = b = 0$ corresponds to the Legendre polynomials F. Olver et al. 2018.

- This basis yields a **sparse**, and in particular, **banded** operator.

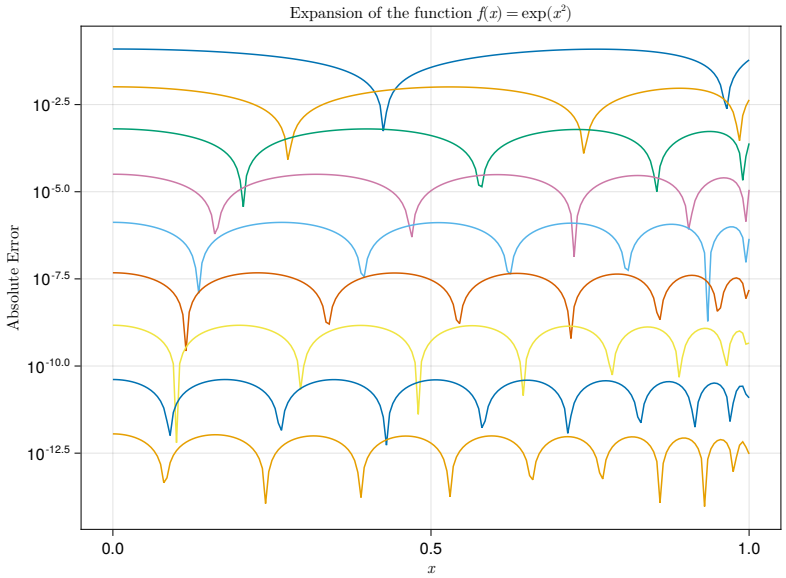

Figure 4.1: Convergence of Jacobi polynomial expansion. Convergence speed according to theory is: TODO.

4.2.11 Definition: Operator

Either the attractive or the repulsive operator can be sparse.
Obtained using [[Theorem 2.16]]. Derivation of the exact row/column form on paper (#include in My Dissertation (cf. **??**))

- [ ] What does the solver look like for other kernels?

4.2.12 Definition: Orthogonal Polynomials

Are univariate polynomials

$$p : \mathbb{R} \mapsto \mathbb{R},\ p(x) = \sum_{k=1}^{N} c_k x^k \,.$$

that form an Orthonormal Basis (cf. **??**) under some inner product.

4.2.13 Definition: Rising Factorial

alias: Pochhammer Symbol
Given by

$$(x)_n = \prod_{k=0}^{n-1} (x + k) \,.$$

4.2.14 Definition: Spectral Convergence

Definition 3.6 (Convergence at spectral speed) An N -point approximation φ_N of a function f converges to f at spectral speed if $|\varphi_N - f|$ decays pointwise in $[-1, 1]$ faster than $O(N^{-p})$ for any $p = 1, 2, ...$ so $p \in \mathbb{N}$.
Source: https://www.damtp.cam.ac.uk/user/cbs31/Teaching_files/c11.pdf.

4.2.15 Definition: Three-Term Recurrence Relationship

All Orthogonal Polynomials (cf. Definition 4.2.12) have (at least) a three-term recurrence relationship.

- [ ] how could I prove that?

4.2.1 Theorem: Integration Theorem that needs a name

On the d-dimensional unit ball B_1 the power law potential, with power $\alpha \in (-d, 2+2m-d)$, $m \in \mathbb{N}_0$ and $\beta > -d$, of the n-th weighted radial Jacobi polynomial

$$(1-|y|^2)^{m-\frac{\alpha+d}{2}} P_n^{(m-\frac{\alpha+d}{2},\frac{d-2}{2})}(2|y|^2-1)$$

reduces to a Gaussian hypergeometric function as follows:

$$\int_{B_1} |x-y|^\beta (1-|y|^2)^{m-\frac{\alpha+d}{2}} P_n^{(m-\frac{\alpha+d}{2},\frac{d-2}{2})}(2|y|^2-1)\mathrm{d}y$$
$$= \frac{\pi^{d/2}\Gamma\left(1+\frac{\beta}{2}\right)\Gamma\left(\frac{\beta+d}{2}\right)\Gamma\left(m+n-\frac{\alpha+d}{2}+1\right)}{\Gamma\left(\frac{d}{2}\right)\Gamma(n+1)\Gamma\left(\frac{\beta}{2}-n+1\right)\Gamma\left(\frac{\beta-\alpha}{2}+m+n+1\right)} {}_2F_1\left(\begin{matrix} n-\frac{\beta}{2}, & -m-n+\frac{\alpha-\beta}{2} \\ \frac{d}{2} & \end{matrix}; |x|^2\right).$$

Theorem 4.2.1 gives an explicit expression for the main integral $Q^\beta : L \mapsto L$, an operator from the Function Space L to the function space L, we are interested in:

$$\hat{Q}^\beta[\rho](x) = \int_{B_1} |x-y|^\beta (1-|y|^2)^{m-\frac{\alpha+d}{2}} P_n^{(m-\frac{\alpha+d}{2},\frac{d-2}{2})}(2|y|^2-1)\mathrm{d}y$$

which is used to construct the Spectral Method Operator Q^β (cf. Definition 4.2.11), acting on the coefficients $\boldsymbol{\rho}$.

4.3 Derivation of Operator

Based on the Three-Term Recurrence Relationship (cf. Definition 4.2.15).

One can even determine an explicit relationship between the coefficients in the Jacobi expansion by considering the Jacobi Matrix (cf. Definition 4.2.9).

Considering the operator $\hat{Q}^\beta[\rho]$ as in Theorem 4.2.1, from the ansatz $\rho(\boldsymbol{x})$ (cf. Definition 4.2.1) we have

$$\hat{Q}^\beta(x) = \sum_{k=0}^{N-1} \rho_k \int_{B_1(\mathbf{0})} \|\boldsymbol{x}-\boldsymbol{y}\|_2^\beta \left(1-\|\boldsymbol{y}\|_2^2\right)^a P_k^{(a,b)}\left(2\|\boldsymbol{y}\|_2^2-1\right) \mathrm{d}\boldsymbol{y}\,. \tag{4.2}$$

We are now interested in a numerical representation of the operator $\hat{Q}^\beta$ acting on the function $\rho \in L^2$, so an equivalent (linear) operator $Q^\beta : \mathbb{R}^N \mapsto \mathbb{R}^N$ acting on the coefficients $\rho_k \in \mathbb{R}$, $k = 1, ..., N$. As every finite-dimensional linear operator must have a matrix representation, we are looking for a $Q^\beta \in \mathbb{R}^{N\times N}$ such that

$$\hat{Q}^\beta[\rho](\boldsymbol{x}) = \boldsymbol{P}_k^{(a,b)}\left(2\|\boldsymbol{x}\|_2^2-1\right)\cdot Q^\beta\boldsymbol{\rho}\,,$$

where $\boldsymbol{P}_k^{(a,b)}\left(2\|\boldsymbol{x}\|_2^2-1\right) \in \mathbb{R}^N$ is the vector of Jacobi polynomials $P_0^{(a,b)}(x)$, $P_1^{(a,b)}(x)$, ..., $P_{N-1}^{(a,b)}(x)$ evaluated at $2\|\boldsymbol{x}\|_2 - 1$ as introduced in and after Definition 4.2.10.

Therefore, starting from Equation (4.2), we obtain

$$\begin{aligned}\hat{Q}^\beta[\rho](\boldsymbol{x}) &= \sum_{k=0}^{N-1}\rho_k\hat{Q}^\beta[wP_k](\boldsymbol{x}) = \sum_{k=0}^{N-1}\rho_k\sum_{j=0}^{N-1} q_{kj}P_k^{(a,b)}\left(2\|\boldsymbol{x}\|_2^2-1\right)\\ &= \sum_{j=0}^{N-1}\sum_{k=0}^{N-1}\rho_k q_{kj}P_k^{(a,b)}\left(2\|\boldsymbol{x}\|_2^2-1\right)\,,\end{aligned}$$

which we will rewrite in matrix-form,

$$\begin{aligned}\hat{Q}^\beta[\rho](\boldsymbol{x}) &= \boldsymbol{P}(\boldsymbol{x})\cdot\begin{pmatrix}\sum_{k=0}^{N-1}\rho_k q_{k,1}\\ \vdots\\ \sum_{k=0}^{N-1}\rho_k q_{k,N}\end{pmatrix} = \boldsymbol{P}(\boldsymbol{x})\cdot\underbrace{\begin{pmatrix}q_{11} & \cdots & q_{1N}\\ \vdots & \ddots & \vdots\\ q_{N1} & \cdots & q_{NN}\end{pmatrix}}_{=:Q^\beta}\begin{pmatrix}\rho_0\\ \vdots\\ \rho_{N-1}\end{pmatrix}\\ &= \boldsymbol{P}_k^{(a,b)}\left(2\|\boldsymbol{x}\|_2^2-1\right)\cdot Q^\beta\boldsymbol{\rho}\end{aligned}$$

where we used $\boldsymbol{P}(\boldsymbol{x}) = \boldsymbol{P}_k^{(a,b)}\left(2\|\boldsymbol{x}\|_2^2-1\right)$ as a shorthand giving us the form of the operator matrix. Each value q_{kj} in it is therefore chosen to satisfy

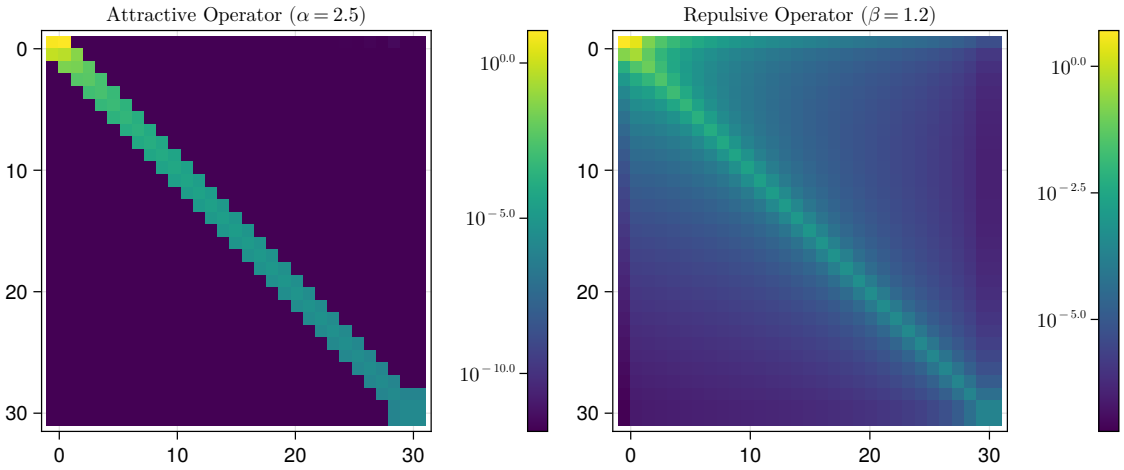

Figure 4.2: The attractive and repulsive operators (matrices), values are in log10-scale.

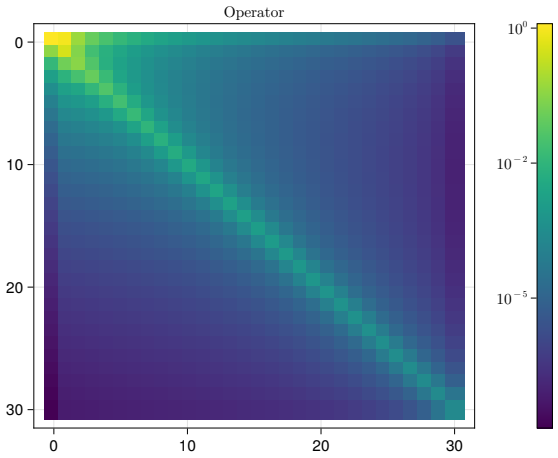

Figure 4.3: Operator

4.4 Results

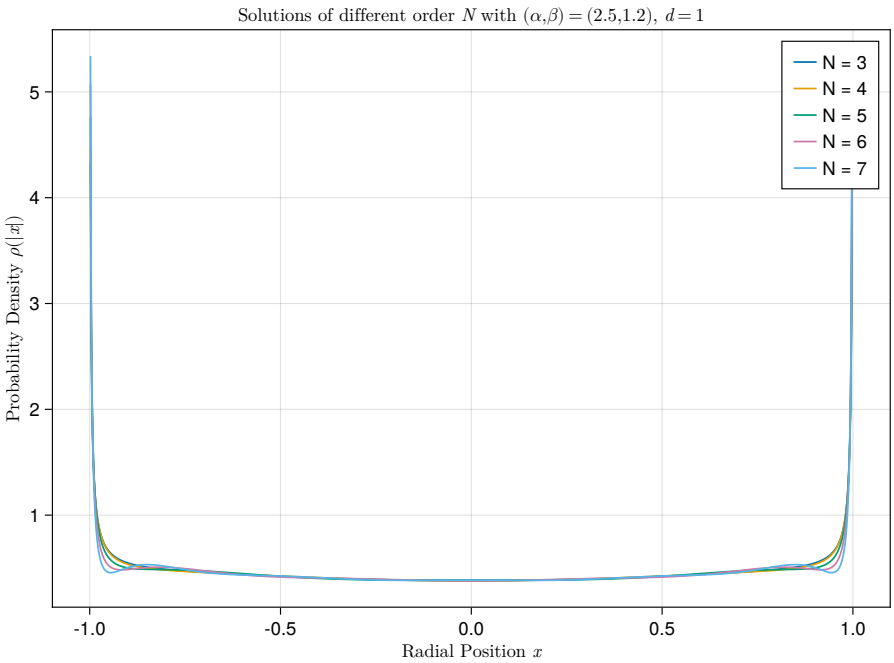

Figure 4.4: Solutions of increasing orders

4.5 Outer Optimisation Routine

Perhaps use [[Clarabel]] if we have a convex optimisation problem?

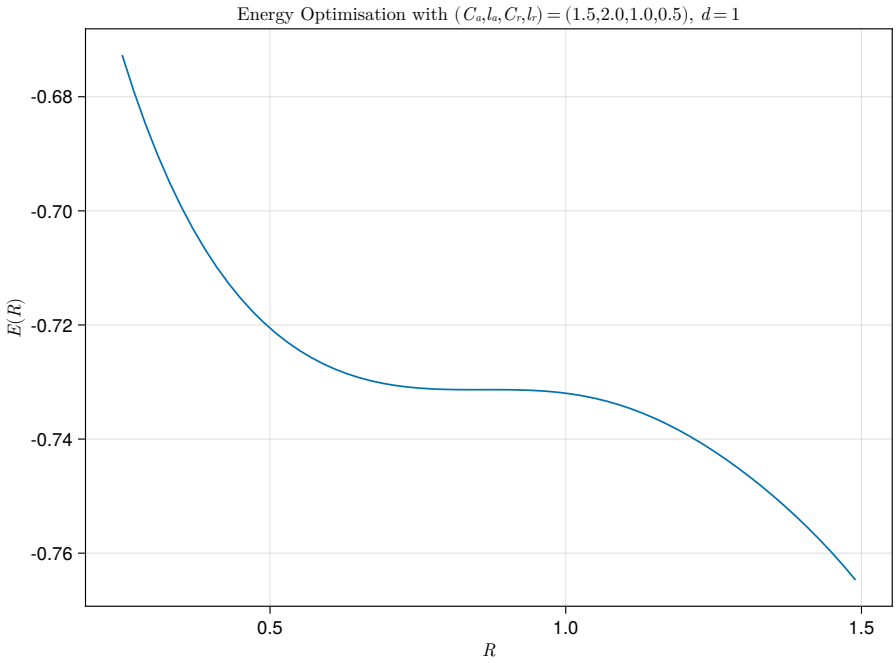

Figure 4.5: Outer Optimisation

4.6 Analytic Solutions

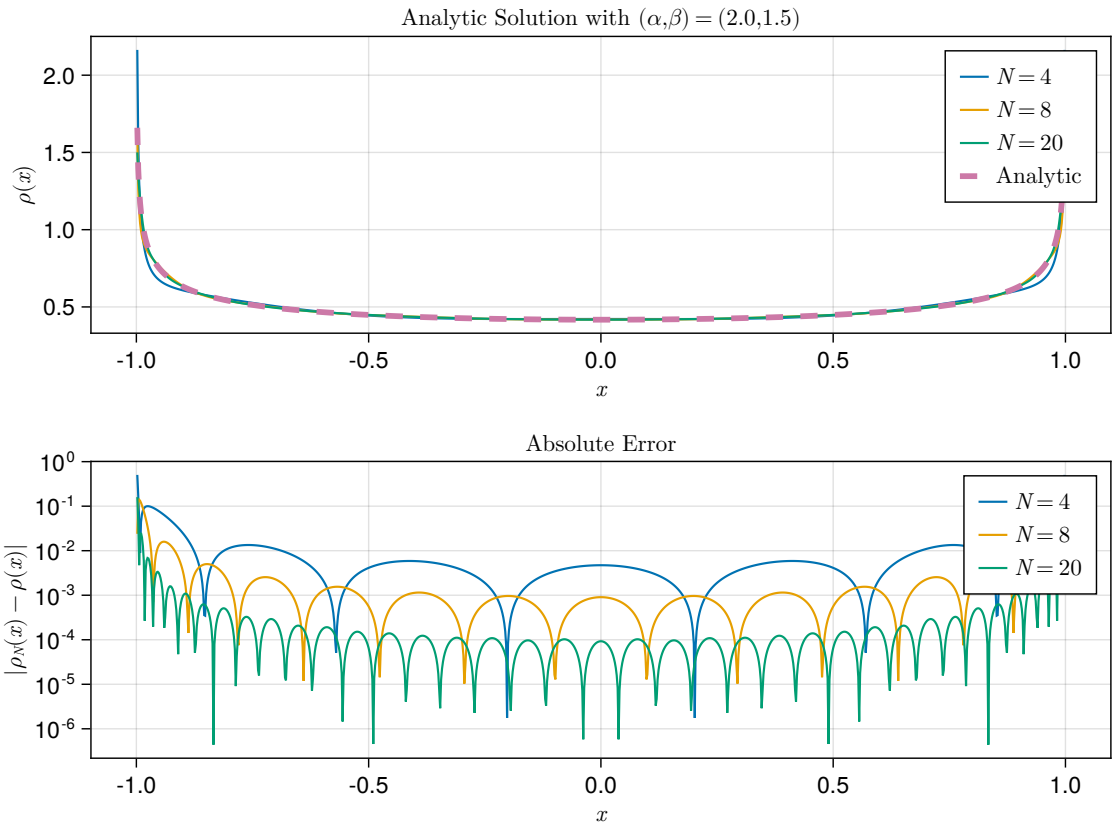

Figure 4.6: Analytic solution and comparison to numerical solutions

4.7 Discussion

- [ ] How does one look at this topic? We should have [[Spectral Convergence]], hopefully.

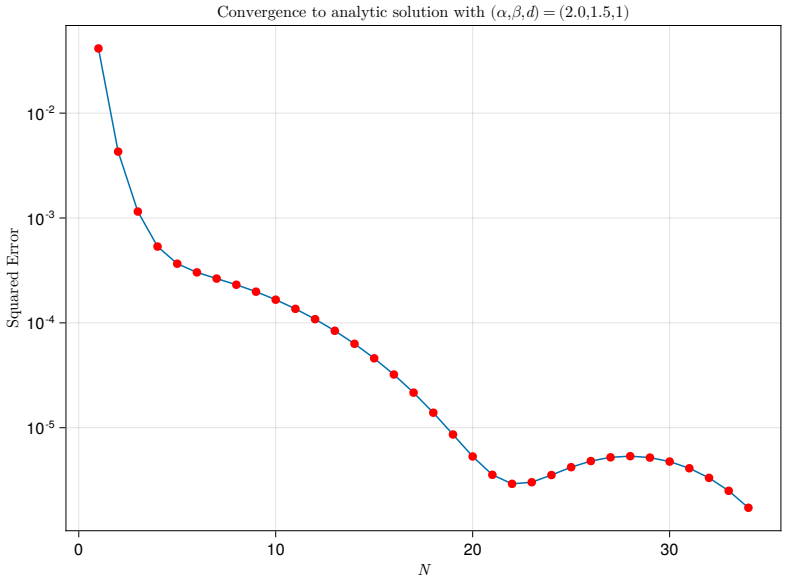

Figure 4.7: Convergence to analytic solutions

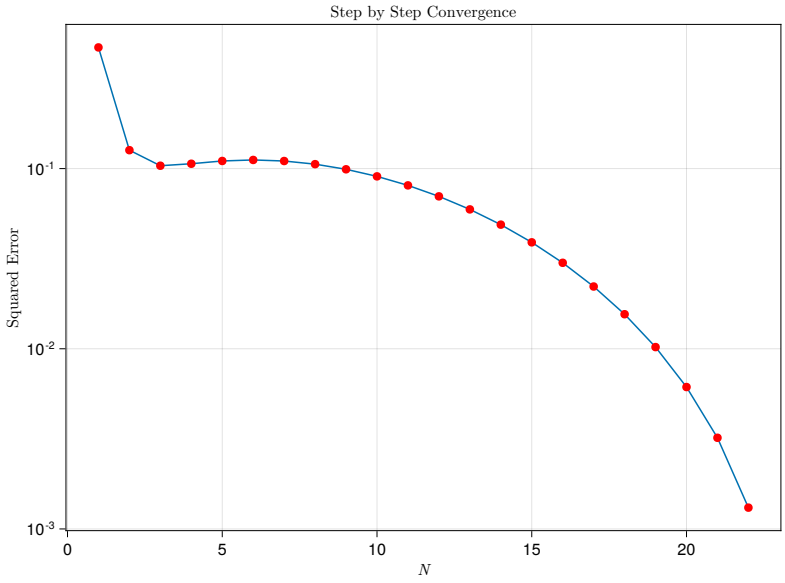

Figure 4.8: Convergence

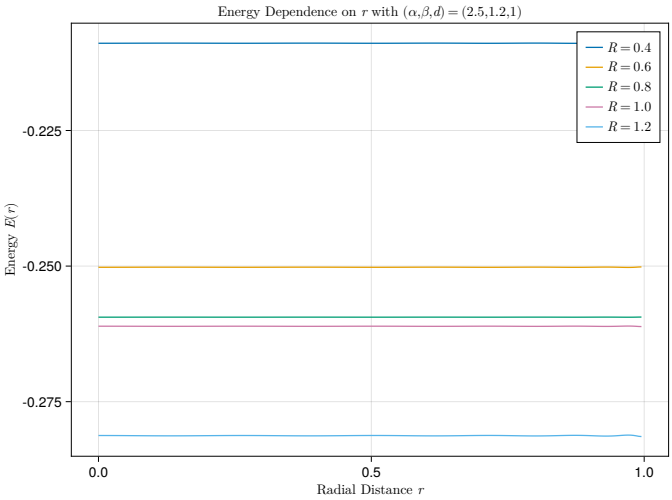

Figure 4.9: Spatial energy dependence on r

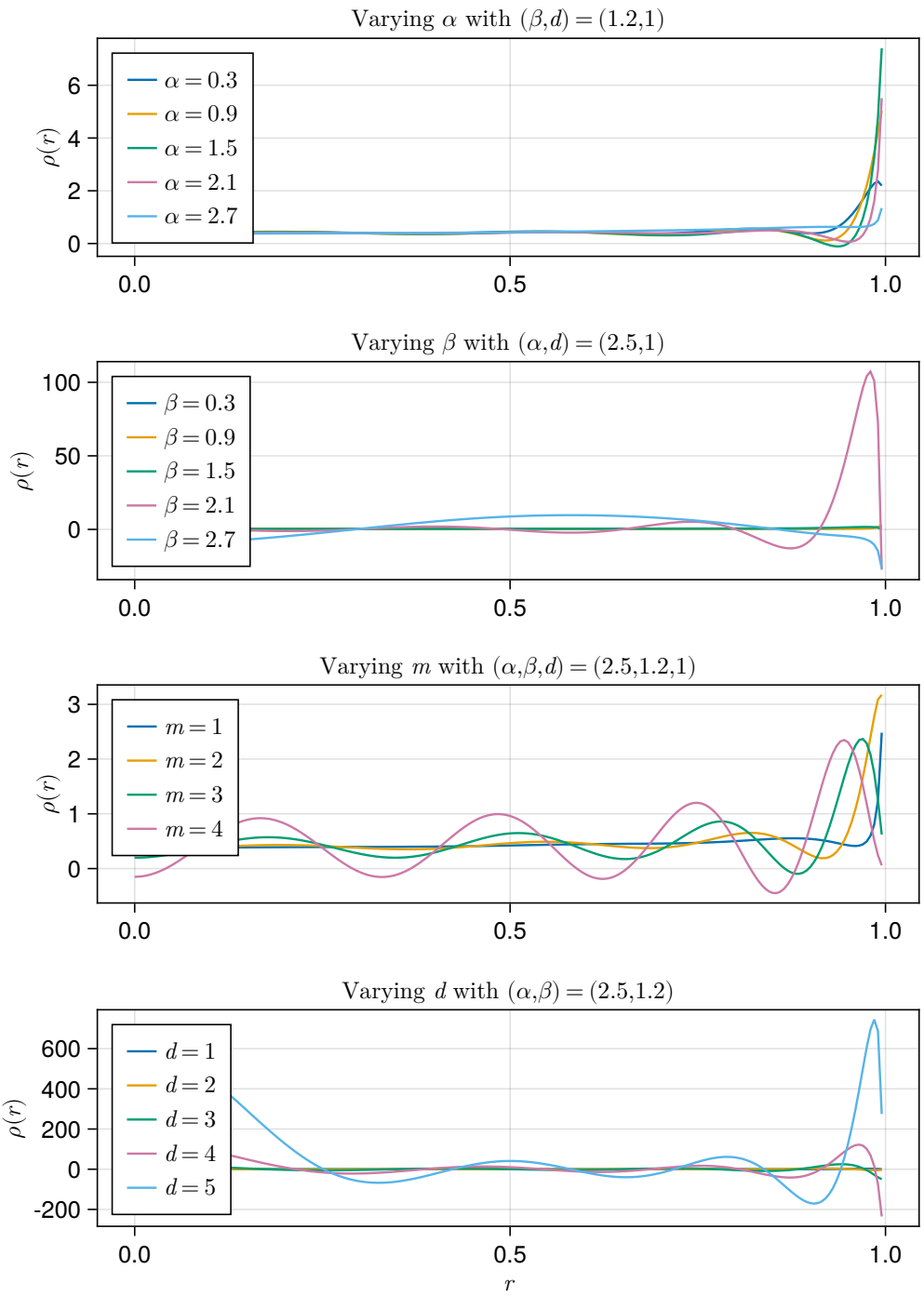

Figure 4.10: Varying parameters in the solver

Chapter 5

General Kernel Spectral Method

is a [[Spectral Method]] involving an [[Integral Equation]].

5.0.1 Structure

- Was ist ein General Kernel?
- How can we expand?
- Mehr Results als im vorigen Chapter [[Spectral Method]]

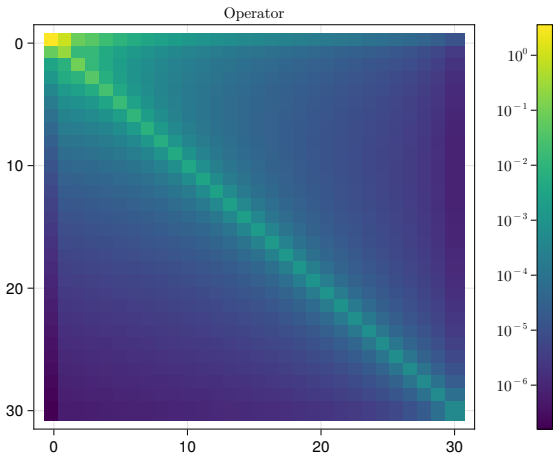

Figure 5.1: Operator

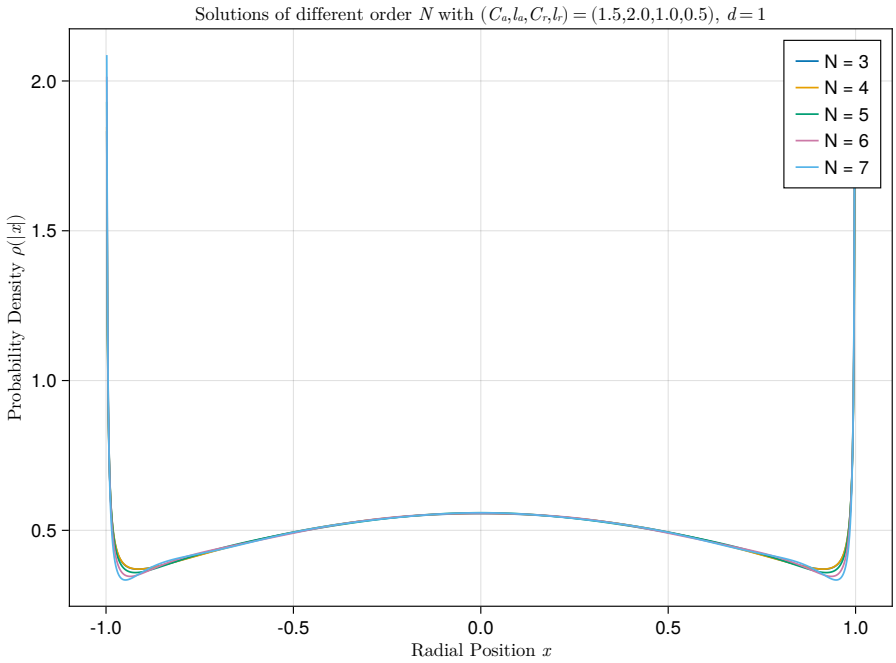

Figure 5.2: Solutions of increasing orders

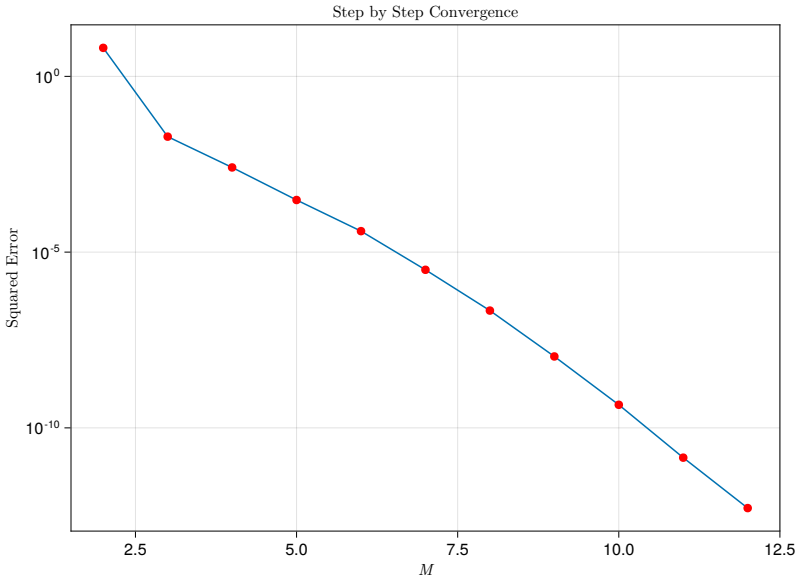

Figure 5.3: Convergence

Chapter 6

Implementation and Results

6.0.1 Structure

- Talk about Julia, C++ and the [[C++ Particle Integrator with GUI]]
- Numerical Results
  - Operator plots
  - Plots of Particle Densities
  - Difference between [[Spectral Method]] and [[Particle Simulator]] results

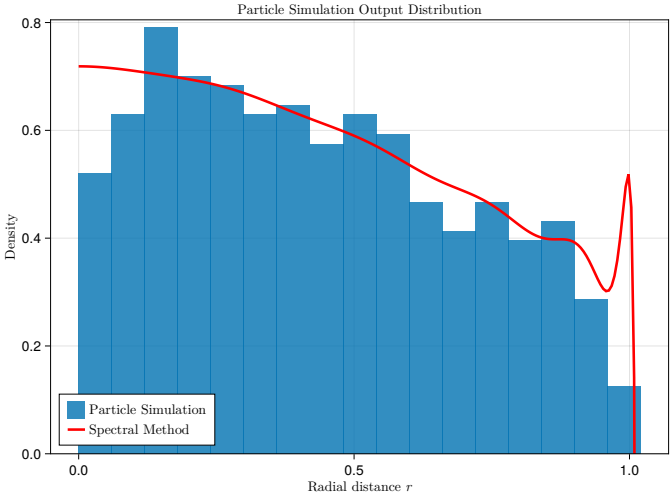

Figure 6.1: Comparison of the radial distance histogram from the simulation output with the solvers equilibrium measure ρ.

Chapter 7

Conclusion

Here we summarise the work that has been presented in this dissertation and discuss possible areas for future work.

7.1 Summary

In the present thesis, we explored the interesting realm of particle-particle interactions. Next to the written part, the reader will find an implementation of the particle simulator, including a GUI, as well as the numerical solver.

Give a summary of what has been done. You might do this chapter by chapter but be sure to highlight all the important points.

7.2 Future Work

You don't actually have to list further work, but most people do this so it seems unusual not to. Just think what you would do next if you had more time on this project.

Other approaches, such as the one in Wu et al. 2015 show that ...

7.3 Conclusion

You might like to give a final conclusion so the reader is left remembering what you have done, rather than what you would do if there wasn't a submission deadline.

Acronyms, Definitions and Theorems

GUI Graphical User Interface 16

Definitions

Theorems

Lemmata

Remarks

Bibliography

Bezanson, Jeff, Alan Edelman, Stefan Karpinski and Viral B Shah (2017). 'Julia: A fresh approach to numerical computing'. In: *SIAM review* 59.1, pp. 65–98. URL: https://doi.org/10.1137/141000671.

Carrillo, José A. and Yanghong Huang (2017). 'Explicit equilibrium solutions for the aggregation equation with power-law potentials'. In: *Kinetic and Related Models* 10.1, pp. 171–192. ISSN: 1937-5093. DOI: 10.3934/krm.2017007.

Cavagna, Andrea, Alessio Cimarelli, Irene Giardina, Giorgio Parisi, Raffaele Santagati, Fabio Stefanini and Massimiliano Viale (June 2010). 'Scale-free correlations in starling flocks'. In: *Proc. Natl. Acad. Sci. U.S.A.* 107.26, pp. 11865–11870. DOI: 10.1073/pnas.1005766107.

D'Orsogna, M. R., Y. L. Chuang, A. L. Bertozzi and L. S. Chayes (Mar. 2006). 'Self-Propelled Particles with Soft-Core Interactions: Patterns, Stability, and Collapse'. In: *Phys. Rev. Lett.* 96.10, p. 104302. ISSN: 1079-7114. DOI: 10.1103/PhysRevLett.96.104302.

D'Orsogna, Maria R. (Dec. 2017). *Why do animals form swarms?* [Online; accessed 12. Aug. 2023]. URL: https://ed.ted.com/lessons/why-do-animals-form-swarms-maria-r-d-orsogna.

Danisch, Simon and Julius Krumbiegel (2021). 'Makie.jl: Flexible high-performance data visualization for Julia'. In: *Journal of Open Source Software* 6.65, p. 3349. DOI: 10.21105/joss.03349. URL: https://doi.org/10.21105/joss.03349.

Gutleb, Timon S., José A. Carrillo and Sheehan Olver (Dec. 2022a). 'Computation of Power Law Equilibrium Measures on Balls of Arbitrary Dimension'. In: *Constr. Approx.*, pp. 1–46. ISSN: 1432-0940. DOI: 10.1007/s00365-022-09606-0.

– (Sept. 2022b). 'Computing equilibrium measures with power law kernels'. In: *Math. Comput.* 91.337, pp. 2247–2281. ISSN: 0025-5718. DOI: 10.1090/mcom/3740.

Olver, F.W.J., A.B.O. Daalhuis, D.W. Lozier, B.I. Schneider, R.F. Boisvert, C.W. Clark, B.R. Miller and B. V. Saunders (eds.) (Dec. 2018). *NIST Digital Library of Mathematical Functions*. http://dlmf.nist.gov. (Visited on 11/11/2020).

Olver, Sheehan and Alex Townsend (Aug. 2013). 'A Fast and Well-Conditioned Spectral Method'. In: *SIAM Rev.* URL: https://epubs.siam.org/doi/10.1137/120865458.

Wu, Lei, Jun Zhang, Jason M. Reese and Yonghao Zhang (Oct. 2015). 'A fast spectral method for the Boltzmann equation for monatomic gas mixtures'. In: *J. Comput. Phys.* 298, pp. 602–621. ISSN: 0021-9991. DOI: 10.1016/j.jcp.2015.06.019.

List of Figures and Tables

List of Figures

List of Tables